# Cyclic Solid-State Multiple Phase Changes with Tuned Photoemission in a Gold Thiolate Coordination Polymer

Oleksandra Veselska, Shefali Vaidya, Chinmoy Das, Nathalie Guillou, Pierre Bordet, Alexandra Fateeva, François Toche, Rodica Chiriac, Gilles Ledoux, Stefan Wuttke, et al.

# Cyclic Solid-State Multiple Phase Changes with Tuned Photoemission in a Gold Thiolate Coordination Polymer

*Oleksandra Veselska, Shefali Vaidya, Chinmoy Das, Nathalie Guillou, Pierre Bordet, Alexandra Fateeva, François Toche, Rodica Chiriac, Gilles Ledoux, Stefan Wuttke, Satoshi Horike, and Aude Demessence**

***Abstract:*** *The discovery of a universal memory that exhibits fast access speed, high-density storage, and non-volatility has fuelled research into phase-change materials over the past decades. In spite of the efficiency of the inorganic chalcogenides for phase-change random access memory (PCRAM), they still have some inherent drawbacks, such as high temperature required for phase change and difficulty to control the domain size of the phase change, because of their brittleness. Here we present a AuI–thiolate coordination polymer which undergoes two successive phase changes on application of mild heating (<200 °C) from amorphous-tocrystalline1- to-crystalline2 phases. These transitions are reversible upon soft hand grinding. More importantly, each phase exhibits different photoluminescent properties for an efficient optical read-out. We believe that the ability of the AuI–thiolate coordination polymer to have reversible phase changes under soft conditions and at the same time to display distinct optical signals, can pave the way for the next generation of PCRAM.*

In today's world, we are creating data at an exponential rate which has driven us to develop super-fast computers for data processing, memory-dense hard drives, and cloud space. In a few years we will be reaching the limit of miniaturization of the existing technology.[1] Pure inorganic materials, like Ge2Sb2Te5, have shown encouraging results as phase-change random access memory (PCRAM), which relies on the change of the electrical resistance of a phase change PC) material between low-resistance crystalline (set) and high-resistance amorphous (reset) states.[2] Nevertheless, these inorganic PC materials require high temperature for the phase change (around 600 °C), meaning a high energy consumption as well. In addition, their intrinsic rigidity and brittleness make the device fabrication challenging.

Coordination polymers (CPs), made of metals and organic linkers, can overcome these limitations and can exhibit low PC temperatures. Indeed, a limited example of CPs show their ability to have thermally induced PC. For example, a gold(I) isocyanide complex exhibits a thermally induced crystal 1-to-crystal 2 through a transient amorphous state,[3] but the process is irreversible and the addition of an organic dopant is required to induce reversibility upon heating. Another ZnII-based CP also shows thermally induced crystalline1-to-amorphous-to-crystalline2 PC, but again no reversibility has been demonstrated.[4] In addition some crystalline CPs have the ability to be amorphized, under either melt quenching or ball milling, but their glass forms are unstable and quickly recrystallized under atmospheric conditions or vapors.[5] In 2015, we reported a solid-state thermally induced, at around 200 °C, amorphous-to crystalline PC in an AuI-based CP, the gold(I) thiophenolate [Au(SPh)]*n*.[6] More importantly, the presence or absence of aurophilic interactions in crystalline and amorphous phases induces different photophysical properties yielding a red and a non-emissive solid, respectively. However, no reversibility has been demonstrated. In addition, we recently reported the ability of some amorphous gold(I)-thiolate, including [Au(SPh)]*n* and [Au(SEtPh)]*n* (SEtPh for 2- phenylethanethiolate), to form transparent glasses, pointing out the softness of these CPs which is important for devices fabrication.[7]

Here, we report an extended work on the [Au(SEtPh)]*n* amorphous phase which undergoes three thermal PC's below 200 °C, including two successive ones in solid state, with resulting phases having different photoluminescence properties and quantum yields. The three new crystalline [Au(SEtPh)]*n* CPs have been fully characterized and the reversibility of amorphous-to-crystalline PC has been demonstrated to highlight their great potential for PCRAM. So this [Au(SEtPh)]*n* system is the first CP that exhibits thermally induced phase changes from amorphous-to-crystalline1- to-crystalline2 with all the phases being stable and having distinct photophysical properties and mechanically induced reversibility.

The synthesis of the amorphous [Au(SEtPh)]*n* phase, from HAuCl4 and an excess of 2-phenylethanethiol (HSEtPh) in methanol at room temperature (RT), has been reported earlier.[7] The DSC experiment under air flow showed that this amorphous phase exhibits a glass transition before the onset of the crystallization at 133 °C to an unknown phase.[7] In this study, extended DSC experiments have been carried out and a second exothermic peak was observed with an onset at 182°C (Figure 1a). Both events correspond to crystallization, named LT (for Low Temperature) and HT (for High Temperature). The two successive crystallizations were confirmed by powder X-ray diffraction (PXRD) measurements (Figure 1b). The amorphous samples were heated in solid state at 100, 120, 140, 160, 180 and 200 °C in an oven under air atmosphere for 12 h and then the PXRD data were measured at RT. The PXRD pattern of the amorphous phase has a broad feature at 6.5° and another less intense one between 20 and 40° in 2$\vartheta$. After the heat treatment at 100 °C, no change was observed on the PXRD pattern. Then, when the amorphous sample is heated at 120–160°C, a crystalline phase with main peaks at 6.7°, 9.5°, 13.5°, 15.1° in 2$\vartheta$ is observed. This crystalline phase corresponds to the LT crystallization event observed on the DSC curve. Next, at higher heating temperatures, between 160 and 200 °C, the diffraction peaks of this LT phase gradually disappear, and new reflections of the HT phase appear (at 5.0°, 9.1°, 10.0°, 11.5° in 2$\vartheta$). Finally, from 200 °C bulk gold appears as result of the decomposition of the HT phase.

The SEM images of the amorphous phase show that it is formed of spherical nanoparticles, homogeneous in size ( ≈75 nm) (Figure 1c and S1). The particles preserve their size and shape once the sample is heated to 120 °C and LT phase is formed (Figure 1d). When the sample is heated to 180 °C and HT phase is formed the particles get a more elongated habit turning from spheres into platelets with length attaining 1 µm (Figure 1e).

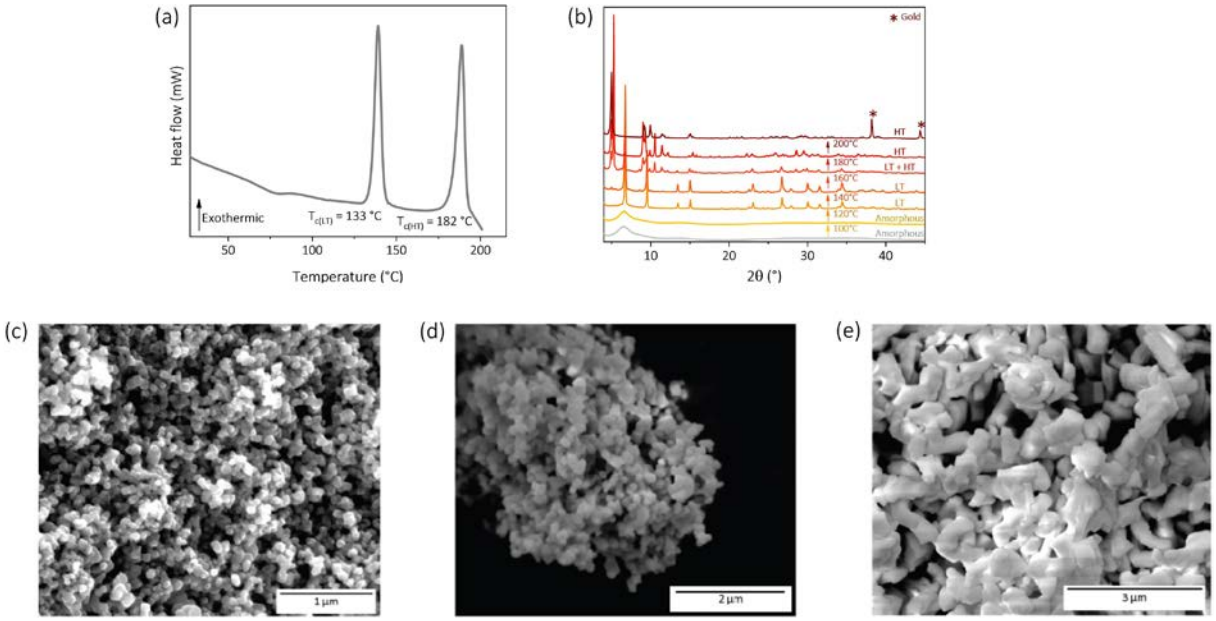


***Figure 1.*** a) DSC analysis carried out under air at 10 °C min 1 of the amorphous phase showing two exothermic peaks of crystallization: LT at 133 °C and HT at 182 °C; b) PXRD patterns measured at RT of six amorphous samples heated in solid state at different temperatures for 12 h (a minor amount of 2D phase is present in the samples obtained by heating at 160 °C and 180 °C: peaks at 5.0° and 10.0°); SEM images of (c) the amorphous phase obtained by direct synthesis, d) LT phase obtained by heating the amorphous phase at 120 °C for 12 h, and e) HT phase obtained

by heating the amorphous phase at 180 °C for 12 h. The structure determination of the LT and HT phases from the PXRD data required high crystallinity and purity of the samples. Thus, the thermal treatment was optimized in order to obtain a powder of acceptable quality. While, good crystallinity of the LT phase was obtained (Figure S2), the attempts targeting pure and highly crystalline HT phase through thermal treatment of the amorphous phase were not successful. Therefore, direct syntheses from the metallic precursor, HAuCl4, and the thiol ligand, HSEtPh, in solvothermal conditions were investigated.[6] The heating of mixture of both metal and organic precursor in DMF in a sealed vial at 80 °C for 1.5 h led to the formation of highly crystalline HT phase. The SEM images of HT phase

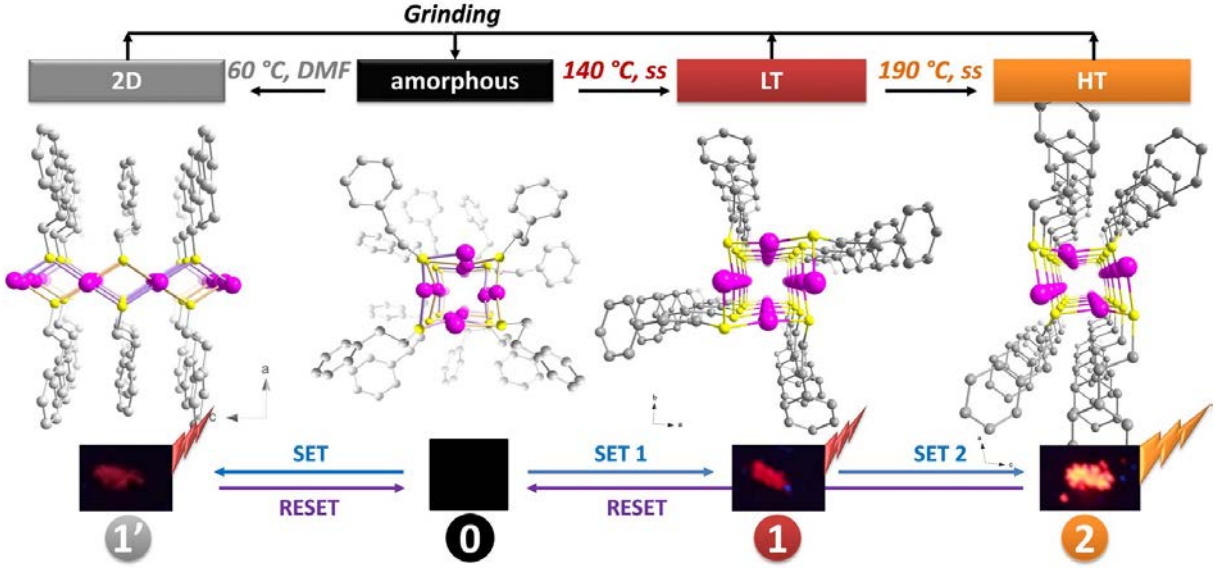


***Scheme 1.*** General representation of the multiple phase changes in [Au(SEtPh)]*n* (*ss* stands for solid state).

obtained by direct synthesis show well defined platelets of 1–2 µm in length (Figure S1). Otherwise, when the starting compounds were mixed in water and heated for 24 h at 120 °C, another crystalline phase is obtained. The PXRD pattern of this phase exhibits predominant (*h*00) reflections at 5.0°, 10.0°, 15.0°, characteristic of lamellar materials. This solid is named 2D phase (PXRD is shown in Figure S2). The 2D phase is formed by needle-like crystallites with length of ≈5 µm and thickness of ≈200 nm (Figure S1). Some reflections of the 2D phase were previously observed as minor impurity in PXRD patterns of samples obtained by heating of the amorphous phase at 160 and 180 °C (Figure 1b). The conditions used for the syntheses of these different phases are described in Scheme 1 (and Scheme S1).

The structures of the three crystalline phases (LT obtained by heating of the amorphous phase, HT and 2D obtained by direct syntheses) were determined from the high resolution PXRD data (Synchrotron SOLEIL, CRISTAL beamline), and are shown in Figure 2 (Figure S3–S5, Table S1).[8] As it has been reported earlier, the amorphous phases of [Au(SPh)]*n* and [Au(SEtPh)]*n* are formed by disorganized double helix of □ S□ Au□ S□ chains.[7] Similarly to [Au(SPh)]*n*,[6] the structure of the amorphous [Au-(SEtPh)]*n* transforms into a crystalline double helix structure upon a thermal treatment (Figure 2). LT crystallizes in the tetragonal *P*42/*n* space group similarly to [Au- (thiomalate)] [9] The –S—Au-- -- chain is composed of two-coordinate gold and µ2-sulfur atoms.

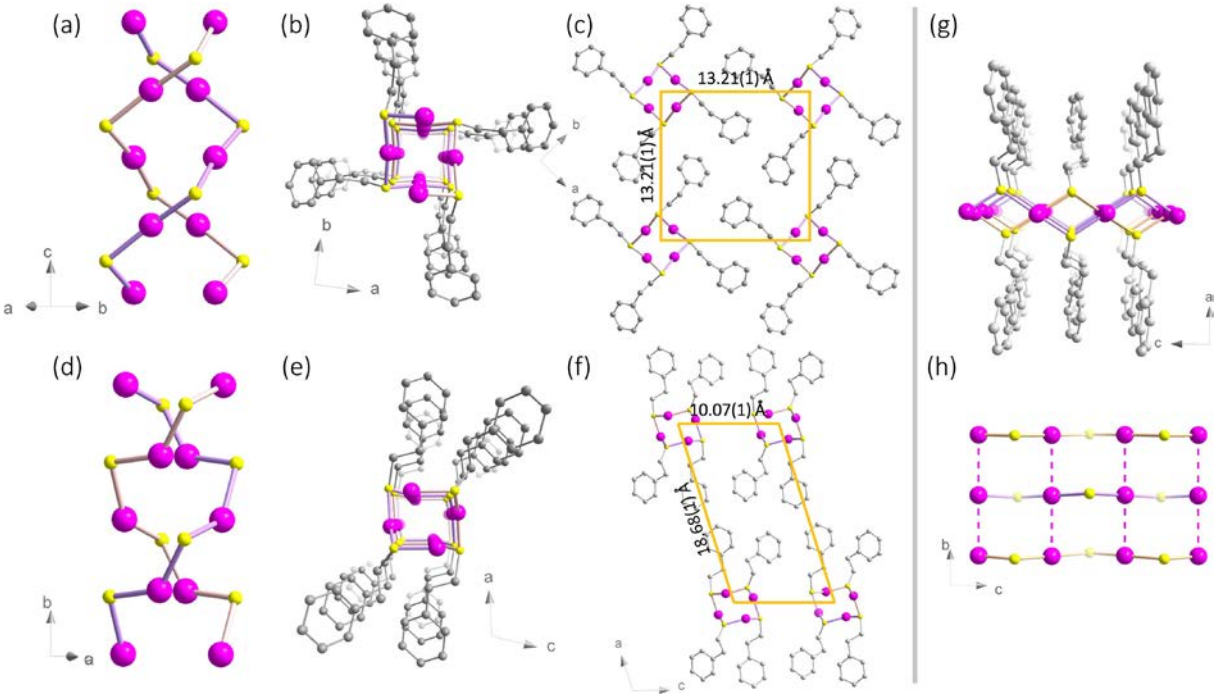


***Figure 2.*** Structure representation of LT phase: a) view on the double helices along *c* axis, b) view in the direction perpendicular to *(ab)* plane and c) packing along *c* axis; and HT phase: d) view on the double helices along *b* axis, e) view in the direction perpendicular to *(ac)* plane and f) packing along *b* axis. The □ Au□ S□ helices and their packing (in orange) form a square in the case of LT phase and a parallelogram in the case of HT phase. Structure representation of 2D phase: g) projection along *b* axis, h) view of the □ S□ Au□ S□ zig-zag chains connected through aurophilic interactions (pink dashed lines). Pink, Au; yellow, S, gray, C. H atoms are omitted for clarity.

The S—Au--S angle of 171.4(4)° is close to linear geometry (Table S2). The interchain Au□ Au distance is 3.44(1) A. Hence, it is at the limit of what can be considered as aurophilic interactions (around 3.5 A).[10] The HT phase crystallizes in the less symmetrical monoclinic *C*2/*c* space group similarly to [Au-(SPh)]*n*. The double interpenetrated helices of □ S□ Au□ S□ are preserved in the structure. Thus, upon

solid state thermally induced PC, the symmetry lowers; it is opposite of what is normally observed in the systems with phase transition (phases of higher symmetry are more stable at higher temperatures).[11] This could be explained by the shortening of some interchain aurophilic interactions down to 3.21(1) A in HT (Figure S6).[7] This results of the bending of S Au S angles in HT to 133(1)° and 137(1)°, compared to the almost linear one in LT (Figure 2, Table S2). This symmetry lowering can also be seen as a distortion of the double helix from square to parallelogram when seen along the chain axis (Figure S6). In addition, the packing of the neighboring helices forms a square with an edge length of 13.21(1) A in LT (Figure 2c) and a parallelogram with edges of 10.07(1) and 18.68(1) A in HT (Figure 2f).

The 2D phase crystallizes in the orthorhombic *Pbca* space group and exhibits a layered structure. The inorganic layer is made of S Au S zig-zag chains that are connected through short aurophilic interactions of 3.05(2) A (Figure 2h and g, Table S2). The gold atoms are in a quasi linear coordination with S Au S angles of 176.8(5)°. The ligand molecules are located in the space between the [AuS]*n* layers without interpenetration. This 2D structure is similar to the one of [Au(*p*-SPhCO2Me)]*n*.[12]

An important structural difference between the three crystalline phases other than the geometry of Au S backbone is the dihedral angles between ethyl and phenyl groups, which are 163(2), 103(10)/148(5) and 174(2)° for LT, HT and 2D phases, respectively (Figure S7). Thus, the ball joint role of the ethyl group favors formation of the different polymorphs.

The FT-IR spectra of all phases show the characteristic bands of aromatic rings and alkane functions (Figure S8). No peak of S H stretching vibration around 2550 cm 1 is observed, confirming the absence of the free ligand and its coordination to the gold atoms via. thiolate groups.

The weight losses of the organic part found from TGA for the three phases, LT, HT and 2D, are in agreement with the expected values, pointing out the purity of the samples (Figure S9). The phases start to decompose under air at 10 °C$min^{-1}$ around 170 °C.

As mentioned above, there is a need for phase changing materials for data storage, with phase change reversibility. Firstly, the PC from amorphous to LT can be induced by heating under air at ≈120 °C (Figure 3), the obtained phase has one exothermic crystallization peak onsetting at 176 °C (Figure S10). Further heating at 180 °C results into HT. No bulk gold formation is observed.

Secondly, to investigate the crystallization processes reversibility, the LT phase, obtained by heat treatment of amorphous phase, was hand grinded for 15 min under ambient atmosphere. That led to the formation of the

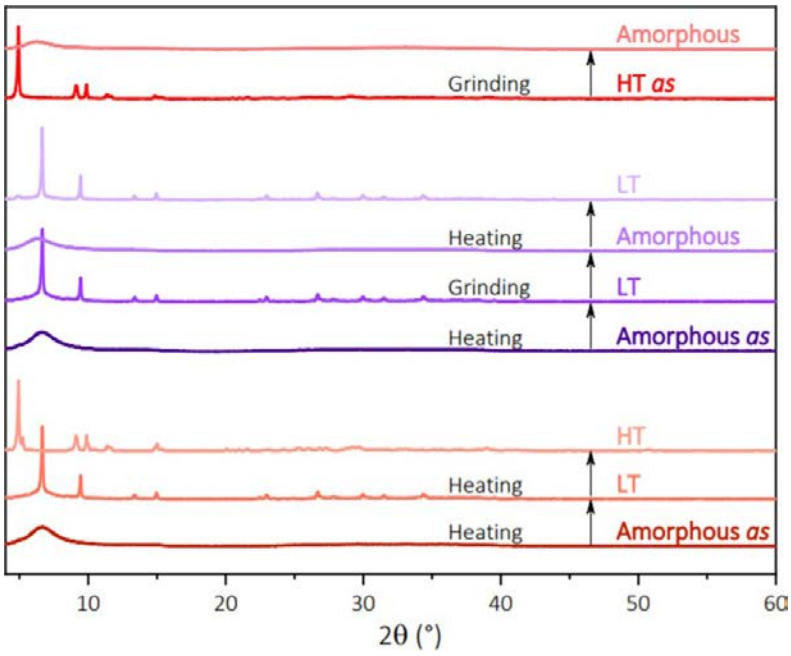


***Figure 3.*** PXRD of the various phases obtained upon heating and grinding performed in order to study the phase changes and their reversibility (*as* for as synthesized).

amorphous phase as confirmed by the disappearance of Bragg peaks and the appearance of a broad diffuse halo at 6° (Figure 3). DSC experiment performed on the so obtained amorphous phase confirms that it can again undergo the crystallization, since it shows two exothermic peaks of crystallization on setting at 137 °C and 167 °C (Figure S10). This points out the possibility of amorphization. The LT phase could be obtained back again by heating the amorphized phase at ≈120 °C (Figure 3). Finally, similar hand grinding experiment was carried out for the HT phase (Figure 3) and the DSC curve of the amorphous phase obtained by grinding HT phase presents also two exothermic peaks on setting at 136 °C and 170 °C (Figure S10). No significant difference of weight loss could be observed on TGA curves between pristine and treated samples, confirming the stability of the material upon grinding (Figure S11).

Heating the amorphous phase in DMF at 60 °C for 18 h led to the 2D phase, which also transforms into the amorphous phase upon grinding (Figure S12a) and as previously observed, the DSC curve of this amorphous phase shows two exothermic peaks corresponding to LT and HT formation (Figure S12b). To the best of our knowledge such switchable solid-state PC phenomenon induced by heating/grinding has not been observed in any CPs till date. Some gold(I) complexes[13] and copper(I) clusters[14] show phase changes, especially upon exposure to mechanical and vapor stimuli, but the use of a liquid in a memory device should be avoided. Hence [Au(SEtPh)]*n* is the first material to show reversibility of the PC upon mild heating and grinding and it can be potentially used in ternary language memory system: Amorphous [0] -> Crystalline LT [1] -> Crystalline HT [2] -> Amorphous [0].

All phases exhibit high-energy absorption, with values in the range $\lambda$abs=250–330 nm for the amorphous, LT and HT phases, and up to 370 nm for the 2D phase (Figure S13), which is assigned to a π-π* transition of the phenyl group.[15] It might originate from the metal-perturbed intra ligand or ligand-to-metal charge-transfer transition as well.[16]

Similarly to [Au(SPh)]*n*,[6] the amorphous [Au(SEtPh)]*n* is not luminescent at RT.[7] However, at RT, the LT phase exhibits a faint red emission (QY≈2%) and the HT phase, an intense red one (QY≈71%). The 2D phase shows faint red emission at RT as well (QY<1%) (Figure 4a).

The photophysical properties of the 1D [Au(SEtPh)]*n* phases (amorphous, LT and HT) are different in terms of QY, but quite similar in emission energies: the amorphous phase has no emission at RT (Figure 4b), but it has its emission maximum at 675 nm at  180 °C, the LT has its maximum at 680 nm at 20°C (685 nm at  180 °C) and the HT at 650 nm at 20 °C (649 nm at  180 °C) (Table S3, Figure S14–S17). In addition, the microsecond range of lifetime decays and the large Stokes shift (>15.000 cm 1) of the three phases are characteristic of a phosphorescent process (Tables S4 and S5, Figure S18–S23). The red emission of gold(I) compounds is usually assigned to a ligand-to-metal charge transfer (LMCT) or a ligand-to-metal- metal charge transfer (LMMCT).[17] The similarity of the emission band positions of the phases suggests that the molecular orbitals involved in the electronic transitions are quite the same. Additionally, the decrease in the QY at RT from HT (≈71%) to LT (≈2%), and to amorphous (0), is probably due, firstly, to the trapping of energy on the defects which are omnipresent in amorphous materials and secondly, to the increase of the aurophilic distances.[18]

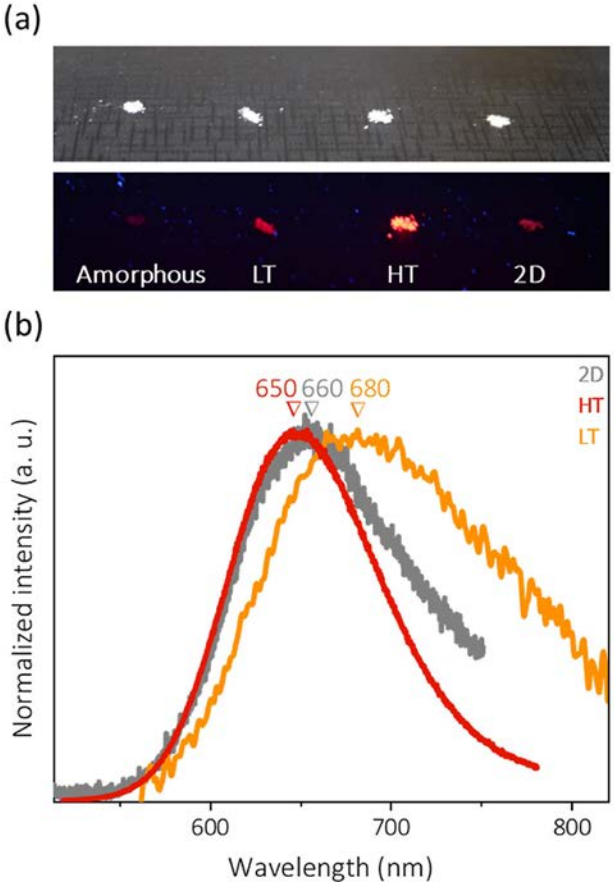


***Figure 4.*** a) Photographs of [Au(SEtPh)]*n* phases under ambient (top) and UV (bottom) light at RT. b) Normalized emission spectra (*λ*ex=300 nm) of [Au(SEtPh)]*n* phases measured at RT.

As discussed above, the CP undergoes reversible PC and each phase has distinct photophysical properties from no emission in amorphous phase to faint emission in the LT phase and to intense emission in HT phase (at RT). Thus, due to these distinct properties and the reversible PC, [Au(SEtPh)]*n* is a potential candidate for new optical PCRAM storage devices using the emission intensity reading.
The 2D phase shows at RT an emission centered at 660 nm and two excitation bands at 308 and 400 nm. At  180 °C additional shoulders appear, for excitation the bands—at 295, 350 and 385 nm and for emission—at 517, 562 and 650 nm (Table S3, Figure S24). Such multiple bands have already been observed in d10 coinage metals thiolate CPs, and have been attributed to additional transitions such as intra-ligand (IL).[12] Indeed, the lifetime decay of this 2D phase is in the microsecond range for the

band centered at 650 nm (*λ*ex=316 nm) and in the nanosecond for the shoulder at 515 nm (*λ*ex=384 nm), pointing out complex processes mixing phosphorescence and fluorescence (Tables S6 and S7, Figure S25–S29).

In summary, it has been shown for the first time the possibility to thermally induce two successive crystallizations from an amorphous gold–thiolate CP, [Au(SEtPh)]*n*, to two crystalline 1D CPs at 133 °C (LT phase) and 182 °C (HT phase) in the solid state. These phase changes are switchable by soft hand grinding to the amorphous phase. In a device the grinding could be replaced by a pressure actuator, that will allow homogeneous applied pressure.[19] More importantly each phase exhibits a different luminescent behavior at RT: the amorphous one is non emissive, LT has faint red emission centered with a QY≈2% and the HT shows an intense red emission with QY≈71%. The distinct photophysical properties are due to, first, the reorganization of the structure into a periodic one and the disappearance of defects upon crystallization of LT and, second, the shortening of aurophilic interactions from LT to HT. Thus, this [Au(SEtPh)]*n* material could be used in optical reading PCRAM with a ternary programming language that allows an increase of memory storage density. Such a kind of reversible PC CP may be a potential sustainable alternative to the inorganic PC materials that are currently used in PCRAM and that require more elevated temperature for the transition, implying the use of cooling-down processes and higher consumption of energy. In addition, the softness of CPs might bring more ductability in the memory devices and allow a better control over the phase change domain that is much harder to perform in the brittle inorganic PC materials.[5b]


### *Acknowledgements*

The authors acknowledge SOLEIL for provision of synchrotron radiation facilities and we would like to thank Erik ELKAIM for assistance in using beamline CRISTAL (Proposal 20150723). This work was supported by the French National Agency (MEMOL project ANR-16-JTIC- 0004-01). A.D. and S.V. acknowledge the CNRS for the EMERGENCE@INC2019 founding (AniMO project). O.V. thanks the Rhone-Alpes region for her PhD grant. O.V. and S.V. thank European Regional Development Fund-Project (No. CZ.02.1.01/0.0/0.0/16_019/0000766). The European Commission is acknowledged by A.D. for the Marie Skłodowska-Curie Individual Fellowship (101031503—Ani- MOC—H2020-MSCA-IF-2020).


### *Conflict of Interest*

The authors declare no conflict of interest.

### *Data Availability Statement*

The data that support the findings of this study are available
in the Supporting Information of this article.


**Keywords:** Coordination Polymers · Gold(I) · Luminescence ·Phase Change



[1] a) S. H. Charap, L. Pu-Ling, H. Yanjun, *IEEE Trans. Magn.* **1997**, *33*, 978; b) L. Abelmann, N. Tas, E. Berenschot, M. Elwenspoek, *Micromachines* **2010**, *1*, 1.

[2] a) M. Wuttig, N. Yamada, *Nat. Mater.* **2007**, *6*, 824; b) S. Raoux, G. W. Burr, M. J. Breitwisch, C. T. Rettner, Y.-C. Chen, R. M. Shelby, M. Salinga, D. Krebs, S.-H. Chen, H.-L. Lung, C. H. Lam, *IBM J. Res. Dev.* **2008**, *52*, 465; c) S. Raoux, W. Welnic, D. Ielmini, *Chem. Rev.* **2010**, *110*, 240; d) R. E. Simpson, P. Fons, A. V. Kolobov, T. Fukaya, M. Krbal, T. Yagi, J. Tominaga, *Nat. Nanotechnol.* **2011**, *6*, 501; e) M. Wuttig, S. Raoux, *Z. Anorg. Allg. Chem.* **2012**, *638*, 2455; f) P. Guo, A. M. Sarangan, I. Agha, *Appl. Sci.* **2019**, *9*, 530.

[3] S. Yagai, T. Seki, H. Aonuma, K. Kawaguchi, T. Karatsu, T. Okura, A. Sakon, H. Uekusa, H. Ito, *Chem. Mater.* **2016**, *28*, 234.

[4] K. Ohara, J. Marti-Rujas, T. Haneda, M. Kawano, D. Hashizume, F. Izumi, M. Fujita, *J. Am. Chem. Soc.* **2009**, *131*, 3860.

[5] a) T. D. Bennett, S. Horike, *Nat. Rev. Mater.* **2018**, *3*, 431; b) S. Horike, S. S. Nagarkar, T. Ogawa, S. Kitagawa, *Angew. Chem. Int. Ed.* **2020**, *59*, 6652; *Angew. Chem.* **2020**, *132*, 6716.

[6] C. Lavenn, L. Okhrimenko, N. Guillou, M. Monge, G. Ledoux, C. Dujardin, R. Chiriac, A. Fateeva, A. Demessence, *J. Mater. Chem. C* **2015**, *3*, 4115.

[7] S. Vaidya, O. Veselska, A. Zhadan, M. Diaz-Lopez, Y. Joly, P. Bordet, N. Guillou, C. Dujardin, G. Ledoux, F. Toche, R. Chiriac, A. Fateeva, S. Horike, A. Demessence, *Chem. Sci.* **2020**, *11*, 6815.

[8] Deposition Numbers 2118145 (for LT phase), 2118149 (for HT phase), and 2118150 (for 2D phase) contain the supplementary crystallographic data for this paper. These data are provided free of charge by the joint Cambridge Crystallographic Data Centre and Fachinformationszentrum Karlsruhe Access Structures service.
[9] R. Bau, *J. Am. Chem. Soc.* **1998**, *120*, 9380.
[10] H. Schmidbaur, A. Schier, *Chem. Soc. Rev.* **2012**, *41*, 370.
[11] J. Zhang, W.-W. Yao, L. Sang, X.-W. Pan, X.-Z. Wang, W.-L. Liu, L. Wang, X.-M. Ren, *Chem. Commun.* **2020**, *56*, 462.
[12] C. Lavenn, N. Guillou, M. Monge, D. Podbevšek, G. Ledoux, A. Fateeva, A. Demessence, *Chem. Commun.* **2016**, *52*, 9063. [13] J. Liang, Z. Chen, L. Xu, J. Wang, J. Yin, G.-A. Yu, Z.-N. Chen, S. H. Liu, *J. Mater. Chem. C* **2014**, *2*, 2243.
[14] R. Utrera-Melero, B. Huitorel, M. Cordier, J.-Y. Mevellec, F. Massuyeau, C. Latouche, C. Martineau-Corcos, S. Perruchas, *Inorg. Chem.* **2020**, *59*, 13607.
[15] J. S. Lim, H. Choi, I. S. Lim, S. B. Park, Y. S. Lee, S. K. Kim, *J. Phys. Chem. A* **2009**, *113*, 10410.
[16] a) C.-H. Li, S. C. F. Kui, I. H. T. Sham, S. S.-Y. Chui, C.-M. Che, *Eur. J. Inorg. Chem.* **2008**, 2421; b) R. Langer, M. Yadav, B. Weinert, D. Fenske, O. Fuhr, *Eur. J. Inorg. Chem.* **2013**, 3623.
[17] E. R. T. Tiekink, J.-G. Kang, *Coord. Chem. Rev.* **2009**, *253*, 1627.
[18] a) J. B. Foley, S. E. Gay, M. J. Vela, B. M. Foxman, A. E. Bruce, M. R. M. Bruce, *Eur. J. Inorg. Chem.* **2007**, 4946; b) L. Rodriguez, M. Ferrer, R. Crehuet, J. Anglada, J. C. Lima, *Inorg. Chem.* **2012**, *51*, 7636.
[19] Y. Dong, J. Zhang, A. Li, J. Gong, B. He, S. Xu, J. Yin, S. H. Liu, B. Z. Tang, *J. Mater. Chem. C* **2020**, *8*, 894.